Integrated Communication and Control Systems: Part II—Design Considerations[1]

Asok Ray
Mem. ASME.

Yoram Halevi
Mechanical Engineering Department,
The Pennsylvania State University,
University Park, PA 16802

Asynchronous time-division multiplexed networks, used in Integrated Communication and Control Systems (ICCS), introduce time-varying and possibly stochastic delays in the feedback control loops. The objective of this on-going research is to develop a comprehensive methodology for the analysis and design of the above class of delayed control systems. In the first part [1] of this two-part paper, we developed a discrete-time, finite-dimensional, time-varying model of the delayed control system; necessary and sufficient conditions for system stability have been established for periodically varying delays. This second part elucidates the significance of the above model relative to the system dynamic performance as well as addresses major criteria for and outlines alternative analytical approaches to ICCS design. Pertinent concepts are illustrated by simulation.

1 Introduction

Integrated Communication and Control Systems (ICCS) essentially belong to a class of distributed digital control for application to complex dynamical processes like advanced aircraft, spacecraft, and autonomous manufacturing plants. System components exchange information via an asynchronous time-division multiplexed network which potentially enhances resource utilization and reduces space, power and wiring requirements of the integrated system. However, multiplexed networks are also a source of time-varying and possibly stochastic delays in the feedback control loop. The objective of this on-going research is to develop a comprehensive methodology for analysis and design of ICCS. This necessitates interactions between the disciplines of communication systems and control systems engineering.

In our earlier work [2, 3], we presented the performance analysis of ICCS networks and demonstrated, by combined discrete-event and continuous-time simulation, how the network-induced delays could degrade the control system performance. In Part I [1], which is a companion paper, we have developed a discrete-time, finite-dimensional, time-varying model of the closed loop ICCS. A necessary and sufficient condition for the stability of delayed control systems with periodically varying delays has been established.

This paper is the second of two parts, and addresses the ICCS design issues for nonperiodic and stochastic delays and outlines the framework of alternative design procedures. Using the model developed in Part I, the impact of network-induced delays on the system stability was investigated, and their physical significance has been exemplified by simulation. The flight control system of an advanced aircraft [3] has been simulated to assess the detrimental effects of a combination of time-varying data latency and mis-synchronization between system components.

The paper is organized in five sections and two appendices. The symbols that were defined in Part I and in this paper are listed in the nomenclature. Section 2 deals with the usage of the model developed in Part I and other criteria for ICCS design. Section 3 presents the simulation results using (1) a simple model to elucidate the intrinsic characteristics of time-varying delayed control systems and (2) a flight control system model of an advanced aircraft to illustrate the detrimental effects of vacant sampling and message rejection at the controller. Alternative analytic procedures for ICCS design are outlined in Section 4. The summary and conclusions of this paper are presented in Section 5 along with recommendations for future research. Appendix A contains a supporting proposition. Appendix B provides a brief description of the network testbed where the experimental evaluation of the ICCS design techniques are planned for this on-going research project.

2 Usage of the Delayed System Model for ICCS Design

In this section we first address the key features of the discrete-time, finite-dimensional, time-varying model of the delayed control system, which was developed in Part I [1]. Then we specify the criteria for avoiding the vacant sampling

[1]This work was supported in part by: National Science Foundation Research Grant No. DMC-8707648.
NASA Lewis Research Center Grant No. NAG 3-823.
Allied Signal Corporation Research Contract No. 81-547792.
[2]Currently at Technion, Haifa, Israel.
Contributed by the Dynamic Systems and Control Division and presented at the Winter Annual Meeting, Chicago, Ill., November 27–December 2, 1988 of THE AMERICAN SOCIETY OF MECHANICAL ENGINEERS. Manuscript received by the Dynamic Systems and Control Division October 1987. Paper No. 88-WA/DSC-2.

and message rejection phenomena from the perspectives of ICCS design.

The augmented state vector $\mathbf{X}$ of the delayed system [1] includes past values of the plant input $\mathbf{u}$ and output $\mathbf{y}$. The amount of the information that must be included in the augmented state vector may change at individual sampling instants because of the time-varying nature of the network-induced delays. This is explained next with reference to the delayed control system model developed in Part I. (The symbols are defined in the nomenclature as well as in Part I.)

The maximum value of the sensor-controller delays Θ_{sc} is $\Delta_s + jT$ if $\delta_{\max} \in [(j-1)T, jT)$ and that of the controller-actuator delay Θ_{ca} is $\delta_p + \delta_{\max}$. Whether these two maxima would occur on the same signal (as it traverses around the control loop) depends on several factors such as the traffic distribution in the network and the relative location of the sensor and controller terminals. In view of the controller-actuator delay, the control input $\mathbf{u}_{k-j}$, generated at the $(k-j)$th controller sample, may arrive at the actuator during the sensor sampling interval $[kT, (k+1)T)$ if $(\Delta_s + \delta_p + \delta_{\max}) \in [jT, (j+1)T)$, and the oldest input that may drive the actuator during the initial part of this interval is $\mathbf{u}_{k-j-1}$. In view of the ICCS design requirements, we consider a special case where each of Δ_s, δ_p and $\delta_{\max}$ is less than T.

(*a*) Since $(\Delta_s + \delta_p + \delta_{\max}) < 3T$ is considered, the first input arriving at the actuator during the interval $[kT, (k+1)T)$ cannot be older than $\mathbf{u}_{k-2}$. Therefore, $\mathbf{u}(t)$ will assume one or more of the four different values, $\mathbf{u}_{k-3}$, $\mathbf{u}_{k-2}$, $\mathbf{u}_{k-1}$ and $\mathbf{u}_k$, during this interval. Similarly, as the maximum of the sensor-controller delay Θ_{sc} is $\Delta_s + T$ for $\delta_{\max} < T$, the oldest sensor data that may be used by the controller in computing $\mathbf{u}_k$ is $\mathbf{y}_{k-1}$.

(*b*) In terms of the derivations of Section 4 of Part I, if $(\Delta_s + \delta_p + \delta_{\max}) < iT$, $i = 1,2,3$, then the maximum number of actuator commands in one sensor sampling period, $l \le i$.

(*c*) If $(\Delta_s + \delta_p + \delta_{\min}) > jT$, $j = 1,2$, then the input matrices $B_m{}^k = 0$ $\forall m \le (j-1)$ and $\forall k$. (See Section 4 in Part I.) In this case, the latest control input that could arrive at the actuator in $[kT, (k+1)T)$ is $\mathbf{u}_{k-j}$ and the input matrices for any subsequent inputs must be zero.

(*d*) Since sensor to controller data latency is assumed to be always less than T, the sensor data $\mathbf{y}_k$ can be used as the latest plant output for generating the inputs $\mathbf{u}_k$ or $\mathbf{u}_{k+1}$ but not for $\mathbf{u}_{k+j}$, $j \ge 2$. Therefore, $p(k) = 0$ or $p(k) = 1$.

(*e*) If $\Delta_s > \delta_{\max}$, then $p(k) = 0$ $\forall k$. In this case $\mathbf{y}_k$ always arrives at the controller *before* the controller sampling instant k.

(*f*) If $\Delta_s \le \delta_{\min}$, then $p(k) = 1$ $\forall k$. In this case $\mathbf{y}_k$ always arrives at the controller *after* the controller sampling instant k.

These observations show that the augmented state vector $\mathbf{X}$, for the general case under observations (*a*) to (*f*), is given as

$$\mathbf{X}_k = [\mathbf{x}_k{}^T \mathbf{y}_{k-1}{}^T \eta_k{}^T \mathbf{u}_{k-1}{}^T \mathbf{u}_{k-2}{}^T \mathbf{u}_{k-3}{}^T]^T \tag{2.1}$$

The above equation indicates the maximum size of $\mathbf{X}$ under the assumption that $(\Delta_s + \delta_p + \delta_{\max}) < 3T$. $\mathbf{X}$ can be reduced in size by eliminating some of the past inputs and outputs under specific conditions. A few examples follow.

If $i = 2$ in observation (*b*), then the term $\mathbf{u}_{k-3}$ is deleted from (2.1); if $i = 1$, then both $\mathbf{u}_{k-3}$ and $\mathbf{u}_{k-2}$ are deleted. If the observation (*e*) holds, then $\mathbf{y}_{k-1}$ should be deleted from (2.1). Observations (*d*) and (*f*) may not specifically reduce the order of the augmented system but some of the time-varying terms are reduced to constants.

Observations (*a*) to (*f*) identify different cases based on $\delta_{\min}$ and $\delta_{\max}$. The sequence $\{p_k\}$, by which the sensor samples are delayed before being processed at the controller, gives rise to four possible cases as described below.

Case #1. Constant Θ_{sc}: *Smaller Delay.* $p(k) = p(k+1) = 0$ implies that the sensor data $\mathbf{y}_k$ and $\mathbf{y}_{k+1}$ reach the controller's receiver before their respective sampling instants. In this case, the sensor data at both instants are subject to a delay of Δ_s before being processed by the controller.

Case #2: Constant Θ_{sc}: *Larger Delay.* $p(k) = p(k+1) = 1$ implies that the sensor data $\mathbf{y}_k$ and $\mathbf{y}_{k+1}$ reach the controller's receiver after their respective sampling instant at the controller. In this case, the sensor data at both instants are subject

Nomenclature for Symbols Used in Parts I and II

$\mathbf{A}$ = plant system matrix $(n \times n)$
$\mathbf{A}_s$ = plant state transition matrix $(n \times n)$
$\mathbf{B}$ = plant input matrix $(n \times m)$
$\mathbf{C}$ = plant output matrix $(r \times n)$
$\mathbf{F}$ = controller system matrix $(q \times q)$
$F(\cdot)$ = probability distribution function
$f(\cdot)$ = probability density function
$\mathbf{G}$ = controller input matrix $(q \times r)$
G = offered traffic
$\mathbf{H}$ = controller output matrix $(m \times q)$
$\mathbf{J}$ = controller direct coupling matrix $(m \times r)$
J = performance index
K = controller gain
P_{mr} = probability of message rejection at the controller's receiver
P_{vs} = probability of vacant sampling at the controller's receiver
p = delay (# of samples) before processing of sensor data starts
$\mathbf{r}$ = reference input $(r \times 1)$
T = nominal sampling period for the sensor and controller
T_c = controller sampling period
T_s = sensor sampling period
t = time
$\mathbf{u}$ = plant input vector $(m \times 1)$
$\mathbf{X}$ = augmented state vector $(N \times l)$
$\mathbf{x}$ = plant state vector $(n \times 1)$
$\mathbf{y}$ = plant output vector, i.e, generated sensor data $(r \times 1)$
$\mathbf{z}$ = delayed sensor data $(r \times 1)$
∇_{sc} = modified sensor-to-controller data latency
Δ_s = time skew between sensor and controller sampling instants
δ_{ca} = controller-to-actuator data latency
$\delta_{\max}$ = supremum of sensor-to-controller data latency
$\delta_{\min}$ = infimum of sensor-to-controller data latency
δ_p = processing delay at the controller computer
δ_{sc} = sensor-to-controller data latency
δ_{ca} = controller-to-actuator data latency
η = controller state vector $(q \times 1)$
θ_a = average delay in the control loop
Θ_{sc} = sensor-controller delay
Θ_{ca} = controller-actuator delay
λ = lumped delay
ρ = maximum # of delayed samples before processing of sensor data
l = maximum # of actuator commands in one sensor sampling period
Φ = augmented system matrix $(N \times N)$

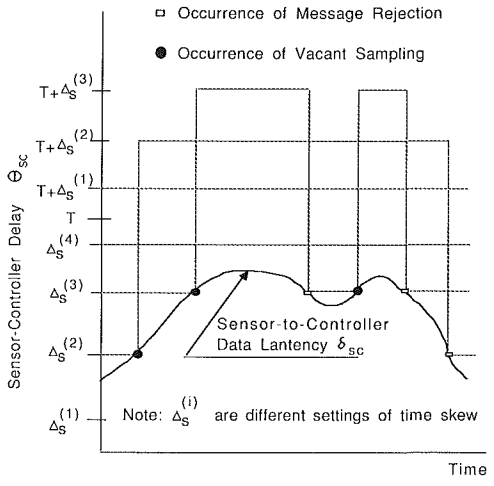

Fig. 1 Impact of time skew on system delay

to a delay of $(T+\Delta_s)$ before being processed by the controller.

Case #3: Message Rejection. $p(k)=1$ and $p(k+1)=0$ imply that the sensor data $\mathbf{y}_k$ and $\mathbf{y}_{k+1}$ reach the controller's receiver after and before the sampling instants k and $k+1$, respectively, at the controller. In this case, both $\mathbf{y}_k$ and $\mathbf{y}_{k+1}$ arrive at the controller's receiver during the $(k+1)$st sample. Since the receiver buffer is assumed to have a capacity of one, $\mathbf{y}_k$ is rejected and $\mathbf{y}_{k+1}$ is retained. This phenomenon has been referred to as *message rejection* in Part I.

Case #4: Vacant Sampling. $p(k)=0$ and $p(k+1)=1$ imply that the sensor data $\mathbf{y}_k$ and $\mathbf{y}_{k+1}$ reach the controller's receiver before and after the sampling instants k and $k+1$, respectively. In this case, no sensor data arrive at the controller during the $(k+1)$st sampling interval. This phenomenon was referred to as *vacant sampling* in Part I. Therefore, in the absence of any new arrival, the controller re-processes the same data $\mathbf{y}_k$ at $k+1$. Thus the control signals $\mathbf{u}_k$ and $\mathbf{u}_{k+1}$ are obtained using the same sensor data $\mathbf{y}_k$. Unless the control law is memoryless, i.e., purely proportional, $\mathbf{u}_{k+1}$ is expected to be different from $\mathbf{u}_k$. The significance of vacant sampling and message rejection is discussed in more detail in the next section by use of a flight control system model of an advanced aircraft.

The above four cases indicate that, for a given network traffic, the time skew Δ_s (between the sensor and controller sampling instants) determines the sensor-controller delay Θ_{sc} in the control loop at every sample. Figure 1 shows how Θ_{sc} could vary for different constant values of Δ_s and a given profile of sensor-to-controller data latency. Thus, Δ_s is a key parameter for the ICCS design.

Even if the sensor and controller sampling periods are designed to be made identical, which is often the case in practice, a certain difference between them always prevails due to the manufacturing tolerance in the clock frequencies resulting in a slow drift in Δ_s. Proposition A.1 in Appendix A shows that, regardless of the exact magnitudes of these tolerances and their probability distribution, Δ_s is uniformly distributed in [0, T) under steady states. Therefore, Δ_s is equally likely to take any value in the [0, T) range, which could be viewed as a constant over a finite time window in the event of a very gradual drift. Since this Δ_s could take the worst possible value in terms of delay and vacant sampling and message rejection, the ICCS design should be robust enough to assure desired stability and performance requirements under these conditions. Usually there is a trade-off between robustness and system performance.

One approach to circumvent the above problem is periodic synchronization of the control system components by which Δ_s is maintained at a desired constant value between 0 and T. Given that Δ_s is a constant parameter, one of the major problems in ICCS design is to determine the optimal value of the constant parameter Δ_s. We discuss this issue in the following paragraph.

The sensor-controller delay δ_{sc} remains a constant at Δ_s if $\Delta_s > \delta_{\max}$ (Case #1) and at $T+\Delta_s$ if $\Delta_s \geq \delta_{\min}$ (Case #2). If the network is lightly loaded, i.e., $\delta_{\max} << T$, a sufficiently small $\Delta_s > \delta_{\max}$ would perhaps satisfy the system stability requirements. However, if the network traffic is moderate to heavy, i.e., $\delta_{\max} \approx T$, or if, as a result of multiple sampling rates, the traffic is light on the average but $\delta_{\max}$ is not small, then the resulting delay of $\Delta_s > \delta_{\max}$ may not be acceptable for a satisfactory system design performance. In that case Δ_s should be selected to be smaller than $\delta_{\max}$, which would cause vacant sampling and message rejection at the controller and δ_{sc} will be either $T+\Delta_s$ or Δ_s depending on whether the sensor-to-controller data latency exceeds Δ_s or not. Apparently, the system dynamic performance depends on the average value of δ_{sc} as well as on the frequency of vacant sampling and message rejection. This is discussed further in Section 4.

So far we have assumed that Δ_s is maintained at a constant desired value by periodic synchronization of the system components. This could be achieved by transmitting high-priority synchronization signals via the network medium or by additional wiring, and would require additional efforts to meet the system reliability requirements. An alternative approach to synchronization is to deliberately assign dissimilar sampling periods to the sensor and the controller. If the sensor sampling period is T_s and that of the controller is T_c such that $T_s = T_c(1-\epsilon)$ for $|\epsilon|<1$, then Δ_s completes a cycle at every $|\epsilon|^{-1}$ samples of the controller. By choosing $|\epsilon|$ sufficiently large (which should still satisfy $|\epsilon| << 1$), Δ_s could be prevented from remaining in the vicinity of the *worst* value for a long time. In other words, the time averaging will reduce the detrimental effects of the worst case. By increasing $|\epsilon|$ either vacant sampling or message rejection (but not both) at the controller can be eliminated. This fact is supported by the following proposition.

Proposition 2.1: The controller receives at least one sensor data during each of its sampling interval provided that

$$\epsilon \geq (\delta_{\max} - \delta_{\min})/T_c \text{ where } \epsilon = (T_c - T_s)/T_c$$

Proof: Let δ^k be the data latency of the kth message from the sensor to controller. The kth sensor data generated at $t_0 + kT_s$ is received at the controller at $t_0 + kT_s + \delta^k$. The next sensor data are received by the controller at $t_0 + (k+1)T_s + \delta^{k+1}$. Therefore, the interval between the reception of two consecutive sensor data, $\Delta T = T_s + \delta^{k+1} - \delta^k$ and Sup $\Delta T = T_s + \delta_{\max} - \delta_{\min}$. Sup ΔT being less than or equal to T_c suffices that the controller always receives at least one sensor data during each of its sampling period.

Corollary to Proposition 2.1: The controller receives at most one sensor data during each of its sampling interval provided that

$$-\epsilon \geq (\delta_{\max} - \delta_{\min})/T_c$$

Proof: Inf $\Delta T = T_s - \delta_{\max} + \delta_{\min}$. Inf ΔT being greater than or equal to T_c suffices that controller always receives at most one sensor data during each of its sampling period.

Remark 2.1: Although no vacant sampling occurs under the condition of Proposition 2.1, some of the sensor messages are rejected at the receiver buffer of controller. Similarly, no sensor message is rejected under the condition of the corollary to Proposition 2.1 but some of the controller sampling periods remain vacant.

Remark 2.2: The average rate of message rejection is equal to that of vacant sampling only if $T_s = T_c$.

3 Simulation of the Delayed Control System

As a first step to ICCS design, a delayed control system was simulated. To elucidate the intrinsic characteristics of the discrete-time, finite-dimensional model, developed in Part I [1], we selected a simple example where the plant model is given as

$$dx/dt = -x + u,\ y = x \tag{3.1}$$

where x, u, and y are scalar functions of time. The control law is chosen to be purely proportional as given by

$$u_k = K(r_k - z_k) \tag{2.2}$$

where r_k is the reference signal, and $z_k = y_{k-p(k)}$ is the delayed sensor data at the controller whose proportional gain is the scalar K. On the basis of the above two equations, the pertinent matrices in (4.9) of Part I reduce to scalars and are set as: $A=-1$, $B=C=1$, $H=0$, $J=K$, and $E_0=1-p(k)$ and $E_1=p(k)$.

For $r_k=0$ and the maximum data latency $\delta_{\max}$ being less than T, the finite-dimensional, discrete-time model of the delayed control system is

$$\begin{bmatrix} x_{k+1} \\ y_k \\ u_k \\ u_{k-1} \end{bmatrix} = \begin{bmatrix} A_s - B_0{}^k K(1-p(k)) & -B_0{}^k Kp(k) & B_1{}^k & B_2{}^k \\ 1 & 0 & 0 & 0 \\ -K(1-p(k)) & -Kp(k) & 0 & 0 \\ 0 & 0 & 1 & 0 \end{bmatrix} \begin{bmatrix} x_k \\ y_{k-1} \\ u_{k-1} \\ u_{k-2} \end{bmatrix} \tag{3.3}$$

where $A_s = \exp(-T)$, $B_0{}^k = 1-\exp(t_0{}^k - T)$, $B_1{}^k = \exp(t_0{}^k - T) - \exp(t_1{}^k - T)$, and $B_2{}^k = \exp(t_1{}^k - T) - \exp(-T)$. The control inputs could arrive at the actuator at the instants $kT+t_0{}^k$ and $kT+t_1{}^k$ during the kth sensor sampling interval $[kT,(k+1)T)$ with the constraint $0 \le t_1{}^k \le t_0{}^k \le T$. This implies that if u_k arrives at the actuator after the $(k+1)$st sensor sampling instant, then $t_0{}^k = T$ and $0 \le t_1{}^k \le T$. Similarly, if u_{k-1} arrives before the kth sensor sampling instant, then $t_1{}^k = 0$ and $0 \le t_0{}^k \le T$.

The significance of the state equation (3.3) under different scenarios is explained below.

No delays: $p(k)=0$ and $t_0{}^k = t_1{}^k = 0$ implying that $B_0{}^k = 1-\exp(-T)$, and $B_1{}^k = B_2{}^k = 0$. Thus, $x_{k+1} = [\exp(-T) - K(1-\exp(-T))]x_k$. This is equivalent to a conventional digital control with a nondelayed feedback.

Delayed Control Signal: $p(k)=0$ or 1, $t_0{}^k = T$ and $0 \le t_1{}^k \le T$. This implies that $B_0{}^k = 0$ and possibly $B_1{}^k \ne 0$ and $B_2{}^k \ne 0$. Therefore, $x_{k+1} = \exp(-T)x_k + B_1{}^k \mathbf{u}_{k-1} + B_2{}^k \mathbf{u}_{k-2}$. This is equivalent to a digital control system where the actuator command is generated using a weighted average of delayed control inputs.

Delayed Control Signal: $p(k)=0$ or 1, $t_0{}^k = T$ and $0 \le r_1{}^k \le T$. This implies that $B_0{}^k = 0$ and possibly $B_1{}^k \ne 0$ and $B_2{}^k \ne 0$. Therefore, $x_{k+1} = \exp(-T)x_k + B_1{}^k \mathbf{u}_{k-1} + B_2{}^k \mathbf{u}_{k-2}$. This is equivalent to a digital control system where the actuator command is generated using a weighted average of delayed control inputs.

Now we present the simulation results of the delayed control system using the following numerical values.

The sampling time and the control signal processing time were set at $T=0.1$ s and $\delta_p = 0.015$ s, respectively. For the purpose of illustrating the effects of periodic delays, the data latencies δ_{sc} and δ_{ca} (in seconds) were chosen to follow sinusoidal profiles with $\omega = 13$ rad/s.

$$\delta_{sc} = 0.015 + 0.005 \sin(\omega t) \tag{3.4a}$$

$$\delta_{ca} = 0.015 + 0.005 \sin(\omega t + \phi) \tag{3.4b}$$

where t is the time in s, and ϕ is the phase differences in rad. However, since $\phi \in [-\pi, \pi)$ depends on several factors including the traffic and relative location of the controller and sensor terminals, we selected $\phi = 0$. In that case, the continuous-time functions in (3.4a) and (3.4b) reduce to discrete sequences by sampling at the sensor and controller sampling instants jT and $jT+\Delta_s$, respectively.

$$\delta_{sc}{}^j = 0.015 + 0.005 \sin(\omega jT) \tag{3.5a}$$

$$\delta_{ca}{}^j = 0.015 + 0.005 \sin(\omega(jT+\Delta_s)) \tag{3.5b}$$

We note, from (3.5a) and (3.5b), that $\delta_{\min} = 0.010$ s, $\delta_{\max} = 0.020$ s. The data latencies $\delta_{sc}{}^j$ and $\delta_{ca}{}^j$ can not be treated as perfectly periodic for the given values of ω and T since there is no finite integer M such that $\delta_{sc}{}^{j+M} = \delta_{sc}{}^j$ and $\delta_{ca}{}^{j+M} = \delta_{ca}{}^j$. Thererefore, the analytical technique, reported in Part I [1] for periodic delays, cannot be readily applied for evaluating the system stability in this case.

A series of simulation runs were conducted to determine the system stability for different combinations of Δ_s and K. Figure 2 shows the stability region of the delayed control system as a function of the feedback gain K and the time skew Δ_s. If $\Delta_s \le \delta_{\min}$, then the sensor-controller delay $\delta_{sc} = T + \Delta_s$; on the other hand, if $\Delta_s > \delta_{\max}$, then $\delta_{sc} = \Delta_s$. Whereas $\Delta_s < \delta_{\min}$ would result in large delays, values of Δ_s in excess of $\delta_{\max}$ may not be desirable as well. In the simulation, we set Δ_s close to $\delta_{\max}$ in the range of 0.019 to 0.020 where stability was maintained for $K=22.5$ with negligible message rejections. Figure 2 shows that values of Δ_s ($< \delta_{\min} = 0.010$) may result in loss of stability even for low gains ($K > 9.5$). If Δ_s cannot be maintained at the desired value, K should be reduced below 9.5 to ensure stability for all Δ_s.

The above problem was partially circumvented by setting the sensor sampling period T_s smaller than the controller sampling period T_c. To show that the improved stability is caused by the fact that $T_c \ne T_s$ and not by a smaller sensor sampling period, T_s was kept constant at the previous value of 0.1 s while T_c was increased. Therefore the relationship $T_c = (1+\epsilon)T_s$, $\epsilon \in [0,1]$ was used instead of $T_s = (1-\epsilon)T_c$. The resulting observations are summarized below.

The rate of sensor message rejection monotonically increases with ϵ. If $T_s \approx T_c$, the time skew Δ_s oscillates between 0

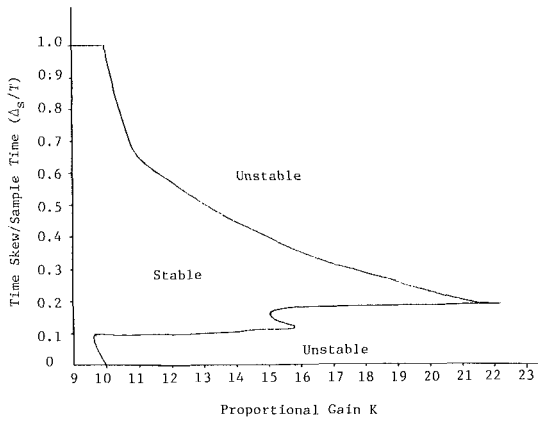

Fig. 2 Stability region

and T_s and the rate of change of Δ_s directly depends on the magnitude of ϵ.

Apparently even small positive values of ϵ could improve stability and, therefore, allow higher gains to achieve a better system dynamic performance. For example, the simulated system was found to be stable at $K=11$ and $\epsilon=0.002$. The simulation results indicate that, for $K \leq 11.5$, the system exhibits stability with ϵ in the range of 0.003 to 0.5. (Values of ϵ in excess of 0.5 were not simulated.) System stability for K in the vicinity of 11.5 is sensitive to small values of ϵ but this sensitivity significantly decreases for larger values of ϵ. At higher K, small ranges of ϵ for which the system is stable may exist but it is apparently difficult to provide physical interpretations of these stability regions from the simulation results only. An analytical method is required for evaluating the bounds of ϵ as a function of the controller parameters, which is one of the areas of the current research.

Better stability with $\epsilon > 0$ results from the reduction of vacant sampling. Loosely speaking, if the system is stable for a wide range of Δ_s, a small decrement in T_s could lead to a stable system; if this range of Δ_s is narrow, changes in T_s have a smaller bearing on the system stability.

We conclude this example by noting that the stability analysis cannot be made solely on the basis of average values of the time-varying delays. This is exemplified below for the case of *identical* sensor and controller sampling periods.

Let the arrival time (relative to the sensor sampling instant) of control inputs $\{u_k\}$ at the actuator be $t_0 = T/2$ and, on the average, one out of three sensor messages arrives at the controller *after* the respective sampling instant. Assuming periodic delays with a period of $6T$, the three different sequences of $p(k)$ (where $z_k = y_{k-p(k)}$) along with the stable ranges of the controller gain K are listed below.

Number	Sequence of $p(k)$	Stable range of K
1	1 0 0 1 0 0	$K<11.1$ and $18.2<K<22.5$
2	1 0 1 0 0 0	$K<18.75$
3	1 1 0 0 0 0	$K<17.5$

While the average system characteristics of the above three sequences are similar, the dynamic behavior of the Sequence #1 is significantly different from those of #2 and #3. This is apparently attributed to the even distribution of delayed sensor arrivals for #1 resulting in relatively more dominant effects of vacant sampling and message rejection. More extensive simulation studies are needed for a better understanding of these phenomena.

Next we investigate the physical phenomena resulting from vacant sampling and message rejection, and assess their detrimental effects on the system dynamic performance. To this effect, the flight control system consisting of the longitudial motion dynamics of an advanced aircraft and a linear time-invariant control algorithm, described in Appendix A of our previous publication [3], was simulated under the following conditions.

- The network access protocol is the SAE Linear Token Passing Bus [4].
- The network medium is shared by 31 terminals.
- Each terminal has a single receiver of queue capacity equal to one.
- The network traffic is periodic with a sampling period of 10 ms for all terminals.
- The terminal #1 operates as both sensor and actuator terminals with its transmitter queue serving the sensor and its receiver queue serving the actuator and the terminal #2 as the controller.
- Every terminal, except the controller terminal, simultaneously generates a message at the beginning of each sample, i.e, the sampling instants of all terminals except the controller are synchronized with the sensor terminal.
- The sensor and controller terminals have a fixed message length with their information part being 64 bit long. The remaining terminals have identical message lengths which depend on the offered traffic.
- Processing delays at the controller is 1 ms.

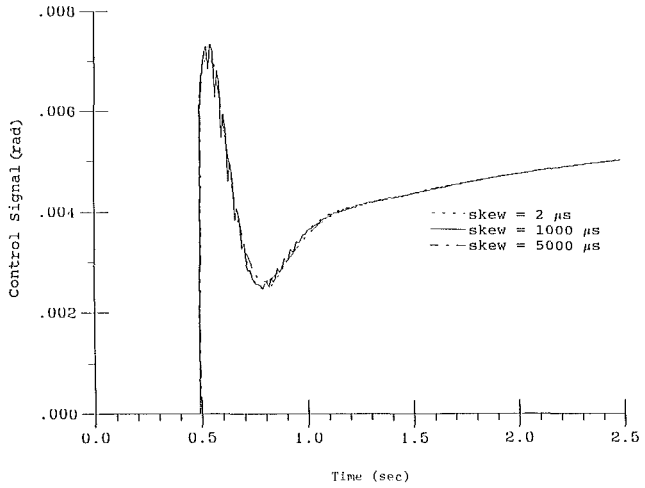

Fig. 3 Distortion of control signal

Our earlier publication [3] prescribed that a network should be designed such that the offered traffic G has a safe margin relative to its critical value G_{cr}. Therefore, G was selected to be 0.2, which is substantially less than the critical value, for conducting simulation runs. (For the condition given above, $G_{cr}=0.993$.)

Three cases with different values of skew Δ_s between the sensor and the controller terminals were considered.

- 5000 μs which is greater than $\delta_{\max}$ (≈ 2000 μs);
- 2 μs which is less than $\delta_{\min}$ (≈ 4 μs);
- 1000 μs which is approximately equal to $(\delta_{\max}+\delta_{\min})/2$.

The simulation run time was selected from 0.5 to 1.5 s, and 100 messages were generated for each terminal at an interval of 10 ms. At $\Delta_s = 5000$ μs, being greater than $\delta_{\max}$, the sensor-controller delay δ_{sc} is always equal to Δ_s. At $\Delta_s = 2$ μs, being less than $\delta_{\min}$, δ_{sc} is always equal to $\Delta_s + T$. In both cases, exactly one sensor data reaches the receiver buffer of controller during every sampling period. At $\Delta_s = 1000$ μs, δ_{sc} would be either Δ_s or $\Delta_s + T$. This fluctuation in δ_{sc} results in vacant sampling and message rejection at the controller.

The transient responses of the control input $u(t)$ at the actuator, as a result of a unit step disturbance in the reference input, is given in Fig. 3 for three different values of Δ_s. When a vacant sample occurs, the control signal is generated on the basis of the sensor data which was used in the previous sample since no fresh sensor data is received during that interval. When the next sensor data arrives at the controller terminal, the control input is derived on the basis of the new data. Figure 3 shows the distortion of the control signal under the above-mentioned transient disturbances for $\Delta_s = 1000$ μs as a result of vacant sampling and message rejection. The distortion of the control input causes high frequency noise in the actuator leading to excessive wear. The distortion may also excite the flexible modes of the aircraft. Implications of vacant sampling and message rejection are explained below.

In view of the four cases of sensor data arrival at the controller, discussed in Section 2, the relationship $\mathbf{z}_k = \mathbf{y}_{k-p(k)}$ between the delayed and true sensor data can be expressed in the following recursive form provided that $p(k)$ is either 0 or 1 $\forall k$.

$$\mathbf{z}_k = \mathbf{z}_{k-1} + [1-p(k)]\Delta\mathbf{y}_k + p(k-1)\Delta\mathbf{y}_{k-1} \tag{3.7}$$

where $\Delta\mathbf{y}_k = \mathbf{y}_k - \mathbf{y}_{k-1}$

The above equation can be interpreted as $\mathbf{z}_k$ being the output of an integrator driven by the first differences $\Delta\mathbf{y}_k$ and $\Delta\mathbf{y}_{k-1}$ generated by the sequence $\{\mathbf{y}_k\}$. If $p(k)=p(k-1)$ as it is in the cases 1 and 2 in Section 2, the input to (3.7) is exactly one of the two first differences. For $p(k)\neq p(k-1)$ implying message rejection or vacant sampling, either both or none of the two first differences are present. In this perspective, the phenomena of message rejection and vacant sampling can be expressed as

$$\mathbf{z}_k = \mathbf{z}_{k-1} + \Delta\mathbf{y}_k + \mathbf{e}_k \tag{3.8}$$

where $\mathbf{e}_k$ represents a train of impulses with varying amplitudes. It is these impulses that distort the control signal sequence $\{u_k\}$ as seen in Fig. 3. In the special case of alternate messages being rejected, the controller response could be worse than that with twice the sample period and no message rejection. The problem of vacant sampling can be partially circumvented by an observer which will provide an estimate of the delayed data. In that case the buffer capacity of the controller's receiver should be increased so that the delayed data can be used for data reconstruction instead of simply being overwritten.

4 Analytical Approach to ICCS Design

The delayed control system model, presented in Part I [1], is time-varying and the currently available tools for analyzing time-varying systems do not offer a practical approach for the ICCS design unless the delays are periodic. For nonperiodic and stochastic delays, an alternative is to base the design procedure on minimizing the average delay in the control loop and the probabilities of vacant sampling and message rejection.

At first we consider the case of the sensor and controller sampling periods being (almost) identical where Δ_s is maintained at a desired constant value. By appropriate selection of Δ_s, the delays in the control loop as well as the probability of vacant sampling may be minimized. This could be achieved without increasing the traffic in contrast to the case where the sensor sampling time is decreased. An analytical approach for selecting the optimal value of Δ_s is outlined below.

Since variations in network traffic pattern are usually slow relative to the dynamics of the control system, the probability distribution of data latency can be considered to be stationary over a sufficiently large period of time. In addition, the assumption of ergodicity allows direct evaluation of the statistical characteristics of data latency from simulation or experimental results. In this way, the probability density function $f_\delta(\cdot)$ of the sensor-to-controller data latency δ_{sc} and controller-to-actuator data latency δ_{ca} can be obtained using the simulation program developed earlier [3]. Similarly, the joint probability density function $f_{\delta\delta}(\cdot,\cdot)$ of ${\delta_{sc}}^k$ and ${\delta_{sc}}^{k+1}$ at two consecutive sensor samples can be generated. (It is important to note that $f_\delta(\xi)\neq 0$ and $f_{\delta\delta}(\theta,\xi)\neq 0$ only if $\theta,\xi\in[\delta_{\min},\delta_{\max}]$). To select an optimal value of Δ_s, the following performance index is minimized.

$$J=(1-\alpha)\phi(\theta_a)+\alpha T P_{vs};\ \alpha\in[0,1] \tag{4.1}$$

where $\theta_a = E[{\Theta_{sc}}^k + {\Theta_{ca}}^k]$ which is the expected value of the total delay in the ICCS loop (see Fig. 2 in Part I), P_{vs} is the probability of vacant sampling at the controller, and ϕ is a given function of θ_a.

Since the sensor and controller have identical sampling frequencies, $P_{vs}=P_{mr}$ which is the probability of message rejection. (See Remark 2.2.)

Several special cases of interest fit into the general performance index.

1. *Minimum average delay:* $\phi(\theta_a)=\theta_a$; $\alpha=0$.
2. *Minimum vacant sampling/message rejection:* $\alpha=1$.
3. *Maximum stability margin:* $\phi(\theta_a)=\varphi_0-\varphi_1$ where φ_0 and φ_1 are the phase margins of the given control system with no delay and a constant delay of θ_a, respectively. The reduction in the phase margin as a result of the additional delay is linear with respect to this delay and is given by $\Delta\varphi=\omega_c\theta_a$ where ω_c is the cross-over frequency of the system which includes the effects of sampling and zero-order-hold. Since $\Delta\varphi$ is proportional to θ_a, this phenomenon is identical to that in the item 1 above. In contrast, the gain margin is a nonlinear function of θ_a. However, the use of phase margin does not preclude the use of a nonlinear function of θ_a to further penalize delays close to the allowable minimum.

Now we consider the case: $\phi(\theta_a)=\theta_a$. Since the controller-actuator delay ${\Theta_{ca}}^k$ is independent of Δ_s, only ${\Theta_{sc}}^k$ in the first term on the right hand side in (4.1) needs to be considered for the optimization procedure.

$$E[{\Theta_{sc}}^k]=\int_{\delta_{\min}}^{\Delta_s}\Delta_s f_\delta(\xi)d\xi+\int_{\Delta_s}^{\delta_{\max}}(\Delta_s+T)f_\delta(\xi)d\xi$$

$$=\Delta_s+T\int_{\Delta_s}^{\delta_{\max}}f_\delta(\xi)d\xi \tag{4.2}$$

The second term P_{vs} in (4.1) is given as

$$P_{vs}=\int_{\delta_{\min}}^{\Delta_s}d\xi\int_{\Delta_s}^{\delta_{\max}}d\phi f_{\delta\delta}(\xi,\phi) \tag{4.3}$$

Using (4.2) and (4.3) in (4.1), sufficient conditions for minimization are obtained by setting $\partial J/\partial\Delta_s=0$ and $\partial^2 J/\partial{\Delta_s}^2>0$ as:

$$(1-\alpha)(1-Tf_\delta(\Delta_s))-\alpha T\int_{\delta_{\min}}^{\Delta_s}f_{\delta\delta}(\xi,\Delta_s)d\xi$$

$$+\alpha T\int_{\Delta_s}^{\delta_{\max}}f_{\delta\delta}(\Delta_s,\phi)d\phi=0 \tag{4.4}$$

and

$$-T(1-\alpha)df_\delta(\Delta_s)/d\Delta_s-\alpha T\int_{\delta_{\min}}^{\Delta_s}\partial f_{\delta\delta}(\xi,\Delta_s)/\partial\Delta_s d\xi$$

$$+\alpha T\int_{\Delta_s}^{\delta_{\max}}\partial f_{\delta\delta}(\Delta_s,\phi)/\partial\Delta_s d\phi-2\alpha T f_{\delta\delta}(\Delta_s,\Delta_s)>0 \tag{4.5}$$

To gain a better insight of the problem, we consider three special cases.

(i) $\alpha=0$: In this case, $\partial J/\partial\Delta_s=0$ yields $f_\delta(\Delta_s)=1/T$ using (4.4) and $\partial^2 J/\partial{\Delta_s}^2>0$ yields $df_\delta(\Delta_s)/d\Delta_s<0$ using (4.5). If the network is not overloaded, implying that $\delta_{\max}-\delta_{\min}<T$, then the density function $f_\delta(\xi)$ must exceed $1/T$ for some ξ. If $f_\delta(\xi)>1/T\ \forall\xi\in(\delta_{\min},\delta_{\max})$, then $\Delta_s=\delta_{\max}$. Figure 4 illustrates these phenomena.

(ii) From (4.3) or directly from Section 2, it follows that $P_{vs}=0$ if $\Delta_s\notin(\delta_{\min},\delta_{\max})$. In these ranges, the Θ_{sc} is held constant at $\delta_{\max}$ if $\Delta_s=\delta_{\max}$.

(iii) If the ICCS network serves a large number of terminals and a majority of them has a stationary random traffic, the sensor-controller delays ${\delta_{sc}}^k$ and ${\delta_{sc}}^{k+1}$ at consecutive samples could be assumed to be independent and identically distributed, i.e., $f_{\delta\delta}(\xi,\phi)=f_\delta(\xi)f_\delta(\phi)$. Then, (4.4) and (4.5) yield less complex expressions for computation of the optimal Δ_s.

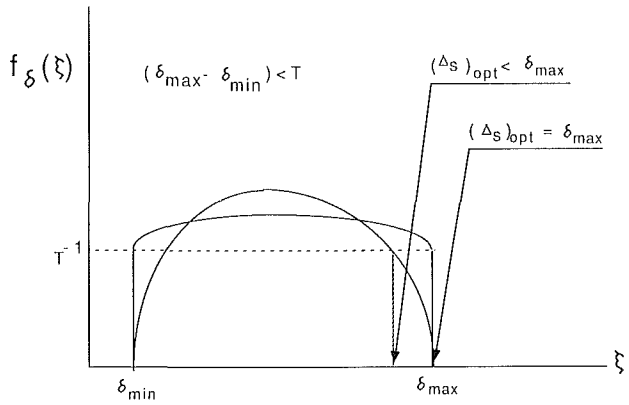

Fig. 4 Optimal time skew

Next we outline the framework of a design approach when the sensor and controller sampling periods are deliberately made different. In this case, Δ_s will vary periodically depending on the design parameter $\epsilon = (T_c - T_s)/T_c$, and the corresponding performance index needs to be minimized with respect to ϵ instead of Δ_s. From the Proposition 2.1 and its Corollary, it follows that $\epsilon > 0$ reduces the probability of vacant sampling and increases that of message rejection. While reduced vacant sampling improves the quality of control signals, message rejections increase the network traffic with ineffective utilization of the resources. Therefore the performance index should be structured in terms of average delay and probabilities of vacant sampling and message rejection as:

$$J = (1-\beta-\gamma)\phi(\theta_a) + \beta T P_{vs} + \gamma T P_{mr} \qquad (4.6)$$

where β and γ are non-negative weights such that $(\beta+\gamma)\epsilon[0,1]$.

From the system design perspectives, the controller sampling period can be maintained constant, and the sensor sampling period T_s be varied to realize perturbations in ϵ. Then the design task is to determine analytical expressions for θ_a, P_{vs}, and P_{mr} as functions of ϵ or T_s. This could be accomplished on the basis of simulated network traffic characteristics. The final step is to evaluate an optimal ϵ using the sufficiency conditions: $\partial J/\partial\epsilon = 0$ and $\partial^2 J/\partial\epsilon^2 > 0$. This is also a subject of the current research.

5 Summary, Conclusions, and Recommendations for Future Work

The paper addresses the design issues of Integrated Communication and Control systems (ICCS) for complex dynamical processes like advanced aircraft, spacecraft, and autonomous manufacturing plants. The ICCS utilize asynchronous time-division multiplexed networking which introduces time-varying and possibly stochastic delays between system components.

One of the major emphases in this paper is on the usage of the discrete-time, finite-dimensional model of the delayed control system which has been developed in Part I [1] for ICCS design. The impact of network delays and possible missynchronization between the sensor and controller was investigated, and their physical significance relative to the system stability has been exemplified. The simulation of the flight dynamics of an advanced aircraft shows that a combination of time-varying data latency in the network and missynchronization between system components could cause *vacant sampling* at the controller and distort the control inputs to the actuator.

Two alternative ICCS design procedures which require a combination of analytical and simulation techniques, have been outlined. Both procedures are based on minimizing a weighted sum of the average time delay in the control loop and the probabilities of message rejection and vacant sampling, and offer the following options: (1) Identical sampling rates of the sensor and controller which are to be periodically synchronized to maintain the desired time skew between their sampling instants; and (2) faster sampling rates for the sensor in order to reduce the occurrence of vacant sampling. Another major research area for analysis and design of ICCS is the parametric evaluation of the system stability under nonperiodic and stochastic delays.

The current research is focused on the development of the above analytical techniques and their verification by combined discrete-event and continuous-time simulation. The next planned phase is to experimentally verify these procedures at the network testbed described in Appendix B.

Acknowledgments

The authors acknowledge the contributions of Messrs. S. H. Hong, L-W. Liou, S. Lee, and R. Luck in this paper.

References

1 Halevi, Y., and Ray, A., "Integrated Communication and Control Systems: Part I—Analysis," published in this issue pp. 00.

2 Ray, A., "Distributed Data Communication Networks for Real-Time Process Control," *Chemical Engineering Communications*, Vol. 65, Mar. 1988, pp. 139-154.

3 Ray, A., "Performance Evaluation of Medium Access Control Protocols for Distributed Digital Avionics," ASME JOURNAL OF DYNAMIC SYSTEMS, MEASUREMENT AND CONTROL, Vol. 109, No. 4, Dec. 1987, pp. 370-377.

4 *SAE Linear Token Passing Multiplex Data Bus*, AS4074.1, Version 3.0, May 1987.

5 *Manufacturing Automation Protocol Reference Specification 2.1A and 2.2*, Society of Manufacturing Engineers, Dearborn, MI, August 1986, and Draft Version 3.0, July 1987.

APPENDIX A

Supporting Proposition

Proposition A.1: Let the clocks of two terminals be synchronized at $t=0$ and their sampling times be $T+\epsilon$ and T, respectively. Then, as $t \to \infty$, the probability distribution of the skew Δ between the terminals is uniform in $[0, T)$ independent of the probability distribution of ϵ provided that ϵ is bounded, i.e., $|\epsilon| < \beta < \infty$.

Proof: Let the random variable $\epsilon \geq 0$ have a probability distribution function $F_\epsilon(x)$ and density function $f_\epsilon(x)$. At the kth sampling instant, the skew $\Delta\epsilon[0,T)$ is given as:

$$\Delta^k = \text{Rem}[k(T+\epsilon) - kT, T] = \text{Rem}[k\epsilon, T]$$

where Rem $[\xi,\phi]$ is the remainder when ξ is divided by ϕ. The distribution function $F_x(x)$ of Δ^k can be expressed in terms of the distribution function $F_\epsilon(x)$ of ϵ as:

$$F_k(x) = P[\Delta^k \leq x] = \sum_{j=0}^{N} P[jT < k\epsilon \leq (jT+x)]$$

$$= \sum_{j=0}^{N} [F_\epsilon((jT+x)/k) - F_\epsilon(jT/k)] \quad \text{for } x\epsilon[0,T) \qquad (A.1)$$

where N = Integer part of $(k\beta/T)$. Differentiating (A.1) with respect to x, we obtain the density function $f_k(x)$, as

$$f_k(x) = (1/k)\sum_{j=0}^{N} f_\epsilon((jT+x)/k),\ x\epsilon[0,T) \qquad (A.2)$$

As $k \to \infty$ (and consequently $N \to \infty$) under steady state conditions, the summation in (A.2) emerges as

$$\lim_{k\to\infty} f_k(x) = 1/T\int_0^{\infty} f_\epsilon(\tau)d\tau = 1/T \text{ for } x\in[0,T) \qquad \text{(A.3)}$$

Hence Δ is uniformly distributed in [0, T) under steady states.

APPENDIX B

Description of the Network Testbed

The 10 Mbps network testbed is designed to experiment with IEEE 802.4 (linear) token passing bus and IEEE 802.2 logical link control protocols in an ISO comptaible network architecture which includes the Transport Protocol (TP) [5]. Under normal operating conditions, the characteristics of IEEE 802.4 are similar to those of SAE linear token passing bus [4].

The testbed is equipped with three terminal interface units, and six host computers including a micro-Vax which can communicate with each other via the network medium or directly using a pair of communication ports. For the ICCS test facility, a tacho-generator and a servomotor function as the sensor and the plant, respectively, and are connected to one microcomputer of the network. Another microcomputer serves as the controller.

A traffic load generator (TLG) has been designed to emulate the scenario of a large number of stations and varying traffic on the network by use of only two terminal interface units. The TLG emulates the major features of the IEEE 802.4 token passing bus protocol. The locations of all odd numbered stations are simulated on the microcomputer host #1 and those of even numbered stations on the microcomputer host #2 where the two microcomputers communicate with each other via the network. The host #1 also provides the A/D and D/A conversion functions for the tacho-generator and the servomotor and is designated as the station #1 in the logical ring of the token passing network of the TLG. The controller is located at host #2 and could be designated with any even station number, i.e., the controller station can be hosted in different positions in the logical ring relative to the sensor/actuator station. Since the host #2 functions as an integral part of the TLG, another microcomputer host #3 is directly connected to host #2. This host #3 provides a multi-processing environment for host #2. The control algorithm is resident in host #3.